

auxiliary anode decreases, the current as a whole increases as another spot is forming elsewhere. At high pressures, because of frequent collisions, the spot can extract electrons from a relatively small region of the plasma resulting in many spots close together while at low pressure this region from which electrons are drawn is large and the spot correspondingly large.

Anode spots will play an important role in those devices in which the currents are large and the anode areas small. They should occur at the anode when the transition from glow to arc is approached and in gaseous discharge devices employing thermionic emitters or cathode spot emitters where the discharge current may become large.

SEPTEMBER 1, 1940

PHYSICAL REVIEW

VOLUME 58

## A Complete Isometric Consistency Chart for the Natural Constants $e$ , $m$ and $h$

JESSE W. M. DUMOND

*California Institute of Technology, Pasadena, California*

(Received December 12, 1939)

The purpose of this paper is to show in greater detail the construction and use of a certain type of consistency chart already briefly described by the author in a previous paper, and by means of it to exhibit, with a few minor changes and some important new additional data, the present status of the dilemma regarding the values of  $e$ ,  $m$  and  $h$  which grows out of the discrepancy between various results of careful measurements of functions of these variables. The discrepancy itself remains practically as glaring and just as unexplained as ever. Scales have been added permitting the values of  $e$ ,  $m$  and  $h$  corresponding to any intersection point to be read off directly.

### THREE-DIMENSIONAL REPRESENTATION

VERY few experiments have been performed which measure any one of the three atomic constants alone without involving one or both of the others. Thus the values of  $e$ ,  $m$  and  $h$  are usually obtained by combining the results of several types of experiment and solving a system of simultaneous equations. There are, however, a great number of ways in which this can be done and these lead to different results so that it becomes desirable to find some graphic representation to exhibit as impartially as possible the inconsistency situation.

In a recent article<sup>1</sup> on the natural constants which will here be referred to as I NC the question of the interconsistency of measurements of functions of the atomic constants  $e$ ,  $m$  and  $h$  was discussed by means of a graphic chart which was essentially an isometric<sup>2</sup> projection of a

three-dimensional plot of the situation. If one thinks of the values of  $e$ ,  $m$  and  $h$  as plotted along the three axes of a three-dimensional rectangular Cartesian coordinate system, then each function of  $e$ ,  $m$  and  $h$  for which some physical experiment yields a numerical value is represented by a surface in this three-dimensional space. Since the functions of  $e$ ,  $m$  and  $h$  determined by experiment are essentially product functions the general equation for such a surface is

$$e^p h^q m^r = A; \quad (1)$$

in which certain of the exponents may, of course, be zero; e.g. the case of the direct determination of  $e$  independent of  $h$  and  $m$  ( $q=0$ ,  $r=0$ ). At least three of these surfaces are required to determine a point  $(e, m, h)$  in this three-dimensional space. With more than three surfaces over-determination may exist and this may be coupled with inconsistency so that various dif-

<sup>1</sup> J. W. M. DuMond, Phys. Rev. **56**, 153 (1939).

<sup>2</sup> Since several different methods of plotting the interconsistency of determinations of functions of  $e$ ,  $m$  and  $h$  have been proposed and R. T. Birge (Phys. Rev. **57**, 250A (1940)) has recently even discussed "an indefinitely large number of variations of such types of chart" it seems

advisable to adopt suitable descriptive names for some of the outstandingly interesting ones. The present author wishes to take such a responsibility only in the case of the type of chart which he originated and he suggests for it the name isometric chart.

ferent points may be determined by the mutual intersection of different triplets of surfaces. The pattern of variously tilted intersecting surfaces in the small region in three-dimensional space in the vicinity of these intersections therefore tells the entire story as to the consistency of the determinations. If all determinations are completely consistent, all the surfaces will intersect in a common point whose coordinates are the values of  $e$ ,  $m$  and  $h$ .

We have said that at least three surfaces are *necessary* to determine a point in this three-dimensional space. *It is important to realize, however, that three such independent surfaces may not be sufficient to determine a point of intersection*, for these surfaces may intersect in a common line rather than in a common point. It is of primary importance therefore to classify the equations corresponding to each type of experiment *into groups having common lines of intersection* for two reasons: first, in order to get a clear picture of what various combinations of the experiments do or do not determine and second, to select, if possible, a most advantageous direction in which to project the entire situation on a plane for the purpose of constructing a two-dimensional chart. It is evident that the way in which a system of equations permits of classification into such groups is a very fundamental absolute property of the system quite independent of any particular geometrical method of representation. The importance of these considerations in connection with the atomic constants seems to have been overlooked in published work up to its recognition in I NC.

The orientation of each surface in space depends on the nature of the function  $e^p h^q m^r$  which it represents, while the numerical value  $A_i$  determined by an experiment fixes the *position* or *location* of the surface (its origin distance if it is a plane). To give symmetry of treatment and freedom from an arbitrary choice of the scales of  $e$ ,  $m$  and  $h$  the author has plotted along the three Cartesian axes not  $e$ ,  $m$  and  $h$  directly but  $(e-e_0)/e_0$ ,  $(m-m_0)/m_0$ ,  $(h-h_0)/h_0$ , where  $e_0$ ,  $m_0$ ,  $h_0$  are values of  $e$ ,  $m$  and  $h$  chosen as an arbitrary reference or origin point for the new chart. So long as this choice of  $e_0$ ,  $m_0$ ,  $h_0$  is judicious so that for the entire region of interest where intersections occur none of the three variables,

$x_e = (e-e_0)/e_0$ ,  $x_m = (m-m_0)/m_0$ ,  $x_h = (h-h_0)/h_0$  ever exceeds, say, 0.5 percent it is obviously possible, by dropping higher order terms, to replace each of the curved surfaces by a plane which will nowhere in the region of interest deviate from the curved surface by an amount appreciable for our purposes.<sup>3</sup> The numerical constants  $A_i$  determined by some particular experiment,  $i$ , are replaced by pure numbers  $a_i = (A_i - A_{i0})/A_{i0}$  where  $A_{i0} = e_0^p h_0^q m_0^r$  and it is then easy to show that Eq. (1) becomes, with neglect of higher order terms

$$px_e + qx_h + rx_m = a_i. \quad (2)$$

Nine such equations which cover all the functions of  $e$ ,  $m$  and  $h$  which to date have been determined by experiments are listed in Table I of I NC.

In I NC experiments 8 ( $A_8 = e/h^3$ ) and 9 ( $A_9 = e^2/h$ ) (the Stefan-Boltzmann radiation constant  $\sigma$  and the fine structure constant  $\alpha$ ) were left out of the discussion because they are much less reliable and accurate than the rest. One of the purposes of this paper, however, is to show a chart provided with scales for including also these determinations if at some later date it should become desirable to do so. Figure 1 of I NC is a perspective view of a three-dimensional model showing six of the nine planes corresponding to determinations 1 to 6 inclusive of Table I of I NC (determination 1 is represented in Fig. 1 of I NC by the base plane). In this model the planes have all been made to pass through the origin to simplify the figure since the purpose at this stage is to discuss merely the *orientations* of the planes. In reality each experimental determination yields a different numerical value  $a_i$

<sup>3</sup> R. A. Beth, Phys. Rev. **54**, 865 (1938) and C. G. Darwin (reference 8) have each proposed plotting logarithms of  $e$ ,  $m$  and  $h$  instead of their natural values, the advantage in doing so being that then the product functions become not approximately but exactly linear functions represented by plane surfaces. I have refrained from following this more elegant procedure for practical reasons. The percent or relative deviations of  $e$ ,  $m$  and  $h$  from the arbitrary values  $e_0 m_0 h_0$  are easily understood at a glance. Scales identical to relative deviation could indeed be obtained by the use of natural logarithms but the great convenience of denary logarithms would then be sacrificed. In practice the relative deviations  $(e-e_0)/e_0$  are very easy to transform into the numerical values  $e$  and vice versa. This can be done very rapidly with ample accuracy on a slide rule, for  $(e-e_0)/e_0$ , of the order 0.5 percent or less, need itself only be known to 0.5 percent accuracy to give an accuracy of 1/40,000 in  $e$ .

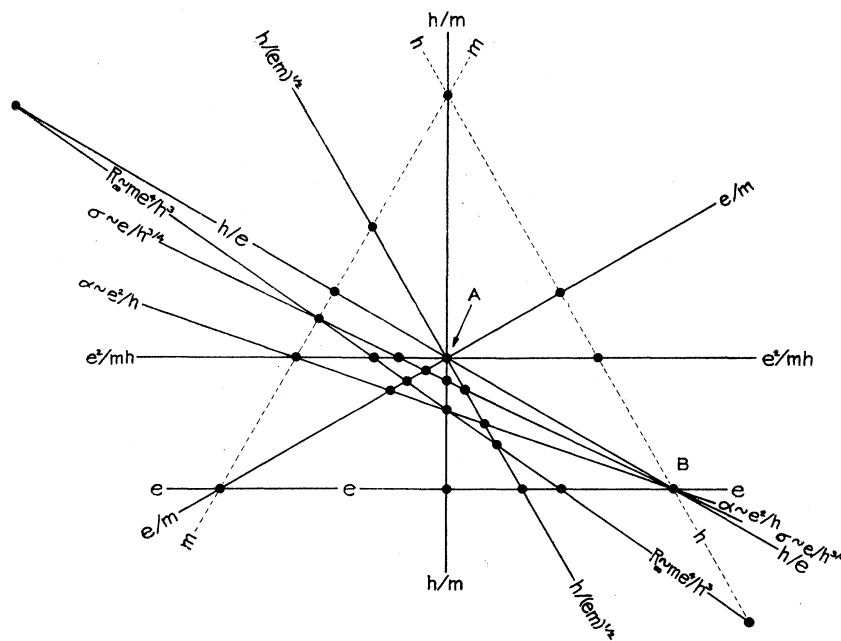


FIG. 1. Graphical representations of cozonal groups. Imagine a three-dimensional rectangular Cartesian coordinate system in which relative deviations of  $e$ ,  $m$  and  $h$  from nearly correct conventional values are plotted to the same scale on the three axes. There are eleven variously orientated planes in this three-dimensional space, nine of which represent the nine functions of  $e$ ,  $m$  and  $h$  which have been determined experimentally, including  $e$  itself. The other two planes (which do not correspond to experimental determinations) are those of  $m$  and  $h$  themselves. For our purpose here only the orientations of the planes concern us, hence they are plotted through a common origin point. This diagram is a *cross section* taken at some arbitrary origin distance through this complex of planes by an "isometric" cutting plane (one making equal angles with the axes of  $e$ ,  $m$  and  $h$ ). Every line on this diagram is the trace of some plane which cuts the isometric plane and the intersection points are the points at which axes common to two or more planes cut the isometric plane. All possible intersection points are shown and this diagram gives, therefore, an exhaustive enumeration of all possible cozonal groups of planes. This diagram is obviously not a consistency diagram.

and its plane must pass not through the origin but at a distance proportional to  $a_i$  therefrom. A scale of  $a_i$ , the percent or relative deviation of the particular experimental result,  $A_i$ , from the origin value,  $A_{i0}$ , may be thought of as provided on the three-dimensional model to facilitate plotting planes representing the individual experimental results.

In the three-dimensional model all planes which pass through a common point represent consistent determinations of functions of  $e$ ,  $m$  and  $h$  and the coordinates of this common point fix the values ( $e$ ,  $m$ ,  $h$ ) upon which these determinations agree.

COZONAL GROUPS ENUMERATED

A striking fact, brought out for the first time in INC, is that *five* out of the seven most im-

portant and accurate types of determinations have planes which are all *parallel to a common line* (the space diagonal making equal angles with the axes  $x_e$ ,  $x_h$  and  $x_m$ ) and which are all, therefore, seen on edge in an isometric projection (projection on a plane normal to the line just referred to, the plane of the hexagon in the prespective view of Fig. 1 of INC). Any group of planes parallel to a common line we shall call a cozonal group. Planes corresponding to experiments 7, 8 and 9 have not been shown in Fig. 1 of INC, to avoid complication. In the present article, Fig. 1, we wish however, in order to effect an exhaustive enumeration of cozonal groups, to show the traces of all nine planes<sup>4</sup> *where these would inter-*

<sup>4</sup>Here also since we are only interested at this point of the discussion in the *orientations* of the planes they are all plotted as though they passed through the origin of the three-dimensional coordinate system.

sect the plane of the hexagon of Fig. 1 of INC. In the same diagram we also show (with dotted lines because they do not stand for experimental determinations) the traces of the planes  $x_h=0$  and  $x_m=0$  where they intersect the plane of the hexagon. We thus obtain a diagram with eleven intersecting lines presenting twenty-five points of intersection. Each of these points of intersection is the point where an axis common to two or more planes in three-space pierces the plane of the hexagon. One sees immediately from Fig. 1 that most of the axes in three-space (intersection points in Fig. 1) have only two or three planes passing through them (lines in Fig. 1). There are two exceptional axes, however, indicated by points marked *A* and *B*, respectively. Five planes pass through each of these. In the case of axis *A* these five planes correspond to experiments 2 to 6, inclusive, all of which are capable of excellent precision<sup>5</sup> and many of which have already received extensive and careful attention from many experimenters. In the case of axis *B*, one of the five planes (*h*) does not represent an experiment at all and two others are very inaccurate experiments corresponding, respectively, to the determination of the Stefan-Boltzmann radiation constant,  $\sigma$ , and to the fine structure<sup>6</sup> constant,  $\alpha$ . Thus for practical purposes axis *B* has only two interesting planes passing through it, the plane of  $h/e$  and the plane of  $e$ . It is evident that Fig. 1 enumerates exhaustively all possible cozonal groups of planes and these are seen to be twenty-five in number, most of which, however, consist of more or less trivial groups of two or three members each. The group *A* is outstanding in that it has five interesting members. While the cross section Fig. 1 is of no use as a chart for indicating the consistency of the determinations, the classification of the equations into cozonal groups is of great value in indicating the exact properties of the system of equations with which we must deal. For example, this chart tells us at a glance that a combination of the measurements of  $R$ ,  $e^2/mh$  and  $h/(em)^{1/2}$  can be solved simultaneously for  $e$ ,  $m$  and  $h$ , while a combination of

the measurements of  $R$ ,  $\alpha$ , and  $h/m$  cannot be used to obtain these constants. The determinant formed of the exponents of  $e$ ,  $m$  and  $h$  vanishes for the second case but not for the first. The lines on the diagram corresponding to the first three functions named have no common intersection point, therefore the planes they stand for are not cozonal and hence they determine a point in space whose coordinates are  $e$ ,  $m$  and  $h$ . The lines standing for the last three functions named are seen to be cozonal since they pass through a common intersection point on the diagram and hence they cannot determine a point in space, but on the contrary they determine only a line. In particular the system of five equations represented by the five lines  $e/m$ ,  $h/e$ ,  $h/m$ ,  $e^2/mh$ ,  $h/(em)^{1/2}$ , which pass through the common point *A*, is insufficient to determine the constants  $e$ ,  $m$  and  $h$ . Only ratios between these constants can be determined by this system. Obviously the properties of any set of equations expressed by the cozonal groups into which they fall are absolute properties of the system independent of any choice of geometrical representation.

#### METHOD OF PROJECTING THE THREE-DIMENSIONAL SITUATION ON A PLANE TO EXHIBIT CONSISTENCY

Each axis represented by the points of Fig. 1 may be considered as a candidate for the direction along which to project the three-dimensional plot for two-dimensional representation. For reasons which will soon be clear, I choose the axis *A* of Fig. 1 for this purpose. Whichever axis is so chosen it is evident that the planes which intersect in, or are parallel to, that axis when projected on a picture plane normal to that axis will be seen on edge and will appear as lines, the traces of the plane in question on the picture plane. From here on for brevity let us call the axis selected for projection simply "the cozonal axis." Now the planes not parallel to this axis (which for brevity we shall call simply the non-cozonal planes) must be treated differently since they are not seen on edge. It so happens with the projection we have just selected that the  $R_\infty$  plane is a noncozonal plane. The author has adopted the procedure of selecting the  $R_\infty$  plane (partly because of the very superior accuracy of

<sup>5</sup> This statement is somewhat less true of experiments 4(a) and (b) than of the rest but these experiments are capable of improvement with further work.

<sup>6</sup> There is some hope through recent theoretical work of J. R. Oppenheimer and his students that the accuracy of the experimental determination of  $\alpha$  may be improved.

this determination) as a standard plane to serve the following very special purpose. *Other non-cozonal planes are represented on our consistency diagram by plotting the projection on the picture plane of the line of intersection in space of each noncozonal plane with the  $R_\infty$  plane.* If we assume an axis in space fixed as to position by a consistent set of cozonal planes, obviously the question of consistency or inconsistency of noncozonal planes with the cozonal set cannot arise *unless there are two or more noncozonal planes which may or may not intersect this axis in the same point.* The necessary and sufficient condition that any two noncozonal planes shall be consistent with any group of two or more consistent cozonal planes is that the line of intersection of the first two shall pass through the line of intersection of the second set. From this it follows that, *on our consistency chart,* the necessary and sufficient condition that any two noncozonal planes shall be consistent with any self-consistent group of cozonal planes is simply that the projection of the line of intersection of the two noncozonal planes shall pass through the intersection of the traces of the consistent cozonal group.

Our chart thus has two kinds of traces on it. (I) Projections of *lines* in three-space on the plane of the chart. These lines in three-space are the intersections of the  $R_\infty$  plane with any other noncozonal plane. The *position* of such lines on the chart depends on two variables, the numerical value of  $R_\infty$  and the numerical value of the other noncozonal function which is involved. Such lines on the chart should therefore be provided with double scales showing the displacements they suffer for changes in either of the two variables while the other is held constant. (II) Lines which are simply the projections of cozonal planes seen on edge but which may, if we wish, also be regarded in the same way as class I, namely as the projections of the line of intersection in space of each cozonal plane with the  $R_\infty$  plane. It is because the cozonal planes are seen on edge that their traces may be regarded as belonging either to class I or II. The position on the chart of such traces of cozonal planes does not vary, however, with variations in  $R_\infty$  and hence only single scales need be attached to represent the displacement which each such line

will suffer when the numerical value associated with its determination is changed. It is well worth noting that the chart of INC which represented all seven of the most interesting types of determinations only needed to have one of these provided with a double scale because of the judicious choice of  $A$  as the axis of projection.

By adhering to *one* standard noncozonal plane (the  $R_\infty$  plane) as the common cutting plane for the remaining noncozonal planes a necessary and sufficient criterion for consistency of a group of noncozonal planes *among themselves* is obtained directly on the two-dimensional chart. If the projections on the picture plane of the respective lines of intersection in space of each member of a group of noncozonal planes with the  $R_\infty$  plane all pass through some cozonal axis (seen projected as a point in the diagram) then these lines in space must not only intersect that axis *but must intersect it at the same point in space,* namely the point where that axis pierces the  $R_\infty$  plane.

It is to be noted that the  $R_\infty$  plane could not serve as the standard cutting plane for the above described purpose if it were parallel to our chosen axis of projection  $A$ .

It may also be added, of course, that only practical considerations of simplicity dictate the choice of the axis  $A$  or indeed of any axis represented by any intersection point in Fig. 1 at all, as the axis of our projection. In principle, any arbitrary direction could have been chosen for the axis of projection but then obviously all planes might be noncozonal and all of them should be supplied with double scales on the chart.<sup>7</sup> The great simplification obtained by the choice of axis  $A$  is thus clear.

C. G. Darwin<sup>8</sup> plots a diagram similar to the author's in which, however,  $e$ ,  $h/e$  and  $e/m$  are selected as the three-dimensional rectangular coordinates, and logarithms are used rather than relative deviations. The axis of projection is normal to the  $e$  plane and on account of the choice of variables this is also the axis cozonal to the principal group of five members which we

<sup>7</sup> The chart devised by R. A. Beth (Phys. Rev. **53**, 681 (1938)) is such a projection, the axis of projection being normal to the  $R_\infty$  plane. No planes are cozonal with this axis. Beth's chart, however, was not provided with double scales so that the effect of the change in  $R_\infty$  could not readily be seen.

<sup>8</sup> C. G. Darwin, Proc. Phys. Soc. London **52**, 202 (1940).

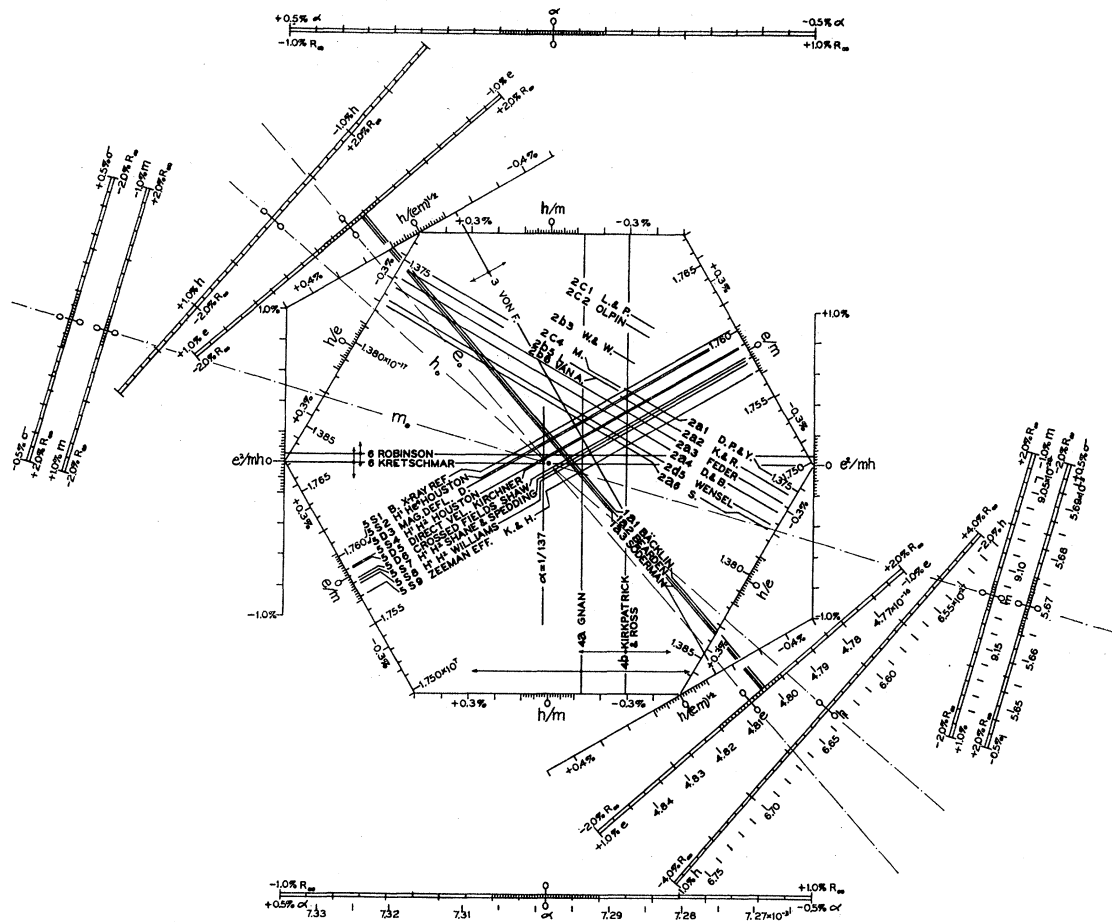


FIG. 2. Complete isometric consistency chart for the nine functions of  $e$ ,  $m$  and  $h$  determined by experiment. The scales for displacement of the lines are expressed in percent deviation from the standard conventional values adopted for the construction of the chart, an intersection in the exact center of the chart indicating that the conventional values  $e_0 m_0 h_0$  are the true ones. In the more interesting cases scales reading directly in terms of these quantities are also attached. Certain of the scales are "double scales," that is, the position of the trace depends on two variables one of which is  $R_\infty$ . Each member of the pair in a double scale shows the displacement that the projected line of intersection of the  $e$  and  $R_\infty$  planes would suffer if the variable of the one scale alone is changed while the other variable is held at its conventional value. A change in both variables then calls for the algebraic sum of the displacements indicated on each scale. The conventional or "origin" values of this chart as well as the experimental values with reference numbers corresponding to those on the chart are listed in Table I.

have here called the cozonal group. Darwin claims that a simplification is obtained by this procedure though it would seem that no greater number of planes are seen on edge by this method than by the more symmetrical isometric projection of the author. Thus if scales of variation were attached to the various lines on Darwin's diagram the same number of double scales would be required as in the isometric chart.

Darwin, in plotting his chart, has followed the procedure of Birge, Dunnington and others of presenting weighted average values for the

various plotted functions of  $e$ ,  $m$  and  $h$ . The author much prefers to exhibit the situation graphically in order to show separately all the reliable independent determinations of each function. Admittedly, this introduces more lines on the graph but it also conveys much more information and permits the reader to use his own judgment more freely. The fact that a point of intersection is the thing to be selected by the reader rather than a line through a number of points (as in the case of the nomographic diagrams of Birge and Bond for example) seems to

the author a distinct advantage if the reader is to be permitted this freedom of choice.

THE COMPLETE ISOMETRIC CHART AND SOME OF ITS ADVANTAGES AND USES

Figure 2 shows such a diagram. On it are given scales for all nine classes of functions of  $e$ ,  $m$  and  $h$  so far determined by experiment. The double scales are easily recognized. They have been drawn with two parallel lines running lengthwise along them to attract the eye. Direct reading scales for each of the variables and functions have been provided as well as the scales of relative or percent deviation from the standard or origin values. In Table I the origin values are given as well as the numerical values for the

different determinations. To use such a chart it is not even necessary to remember the principle of its construction. Each trace is merely to be plotted between its two parallel scales at the percent deviation (plus or minus) from the origin value called for by the experimental value obtained. (Or it may be plotted directly by means of the direct reading scales.) Those traces which intersect in the same point represent mutually consistent determinations. The values of  $e$ ,  $m$  and  $h$  upon which such mutually consistent traces agree can be read off immediately on the scales of  $e$ ,  $m$  and  $h$  either directly or in terms of percent deviation from the origin values  $e_0 m_0 h_0$ . This operation is slightly facilitated by drawing the origin traces through the zeros of the percent

TABLE I. Conventional or origin values used in isometric chart.

$e_0 = 4.80650 \times 10^{-10}$  e.s.u.,  $m_0 = 9.11780 \times 10^{-28}$  gram,  $h_0 = 6.63428 \times 10^{-27}$  erg sec. and in consequence:  
 $e_0/m_0 = 1.75850 \times 10^7$  e.m.u./gram,  $h_0/e_0 = 1.38028 \times 10^{-17}$  e.s.u.,  $h_0/m_0 = 7.27621$   
 $e_0^2/(h_0 m_0) = 3.81921 \times 10^{34}$ ,  $h_0/(e_0 m_0)^{1/2} = 1.00216 \times 10^{-8}$ ,  $R_\infty = 2\pi^2 e^2 c^{-2} (h/e)^{-3} (e/m) = 109,737 \text{ cm}^{-1}$   
 $c = 2.99776 \times 10^{10}$  cm/sec.,  $\alpha_0 = 7.29870 \times 10^{-3}$ ,  $\sigma_0 = 5.67122 \times 10^{-5}$  erg  $\text{cm}^{-2}$  deg. $^{-4}$  sec. $^{-1}$

Experimental values used in isometric chart

QUANTITY DETERMINED	VALUE	SYMBOLS ON CHART	METHOD	OBSERVER	REFERENCE	RECOMPUTED BY	
$e$	$4.8016 \times 10^{-10}$	1 a 1	Ruled grating and crystal x-ray diffraction	E. Bäcklin	Zeits. f. Physik <b>93</b> , 450 (1935)	Birge (1939 letter)	
	4.8022	1 a 2		J. Bearden	Phys. Rev. <b>37</b> , 1210 (1931); <b>47</b> , 883; <b>48</b> , 385 (1935)	Birge (1939 letter)	
$h/e$	4.8026	1 a 3	Continuous x-ray spectrum limit	M. Söderman	Nature <b>135</b> , 67 (1935)	Birge (1939 letter)	
	$1.37494 \times 10^{-17}$	2 a 1		Duane, Palmer and Yeh	J. Opt. Soc. Am. <b>5</b> , 376 (1921)	DuMond	
	1.37541	2 a 2		P. Kirkpatrick and P. A. Ross	Phys. Rev. <b>45</b> , 454 (1934)	"	
	1.37588	2 a 3	Continuous x-ray spectrum limit	H. Feder	Ann. d. Physik <b>51</b> , 497 (1929)	"	
	1.37646	2 a 4		J. W. M. DuMond and V. Bollman	Phys. Rev. <b>51</b> , 400 (1937)	"	
	1.3772	2 a 5		$c_2$ optical pyrometry	H. T. Wensel	J. Research Nat. Bur. Stand. <b>22</b> , 386, 387 (1939)	Wensel
	1.3775	2 a 6		G. Schaitberger	Ann. d. Physik <b>24</b> , 84 (1935)	DuMond	
	1.3715	2 c 1	Photoelectric effect	P. Lukirsky and S. Prilezaev	Zeits. f. Physik <b>49</b> , 238 (1928)	"	
	1.372	2 c 2		A. R. Olpin	Phys. Rev. <b>36</b> , 251 (1930)	"	
	1.3736	2 b 3	Critical potentials	R. Whiddington and E. G. Woodroffe	Phil. Mag. <b>20</b> , 1109 (1935)	"	
	1.375	2 c 4		R. A. Millikan	<i>Electrons (+ and -), Protons, Photons, Neutrons, and Cosmic Rays</i> (U. of Chicago), p. 242 (1934)	"	
	1.3752	2 b 5	Critical potentials	E. O. Lawrence	Phys. Rev. <b>28</b> , 947 (1926)	"	
	1.3752	2 b 6	Critical potentials	L. C. Van Atta	Phys. Rev. <b>38</b> , 876 (1931); <b>39</b> , 1012 (1932)	"	
$h/(em)^{1/2}$	$1.00079 \times 10^{-8}$	3	Electron $\lambda$ and voltage	S. von Friesen	Proc. Roy. Soc. <b>A160</b> , 424 (1937) also Inaugural Diss. Uppsala 1936	"	
$h/m$	7.267	4 a	Electron $\lambda$ and velocity Compton shift	J. Gnan	Ann. d. Physik [5] <b>20</b> , 361 (1934)	Kirchner	
	7.255	4 b		P. Kirkpatrick and P. A. Ross	Phys. Rev. <b>45</b> , 223 (1934)	"	
$e/m$	$1.7602 \times 10^7$	5 s 1	X-ray refraction in diamond	J. A. Bearden	Phys. Rev. <b>54</b> , 698 (1938)	Birge (1939 letter)	
	1.7600	5 s 2	Spectroscopic H <sup>1</sup> He <sup>4</sup>	W. Houston	Phys. Rev. <b>30</b> , 608 (1927)	"	
	1.7598	5 d 3	Magnetic deflection	F. Dunnington	Phys. Rev. <b>52</b> , 498 (1937)	"	
	1.7590	5 s 4	Spectroscopic H <sup>1</sup> H <sup>2</sup>	W. Houston	Phys. Rev. <b>51</b> , 446 (1937); <b>55</b> , 423 (1939)	"	
	1.7590	5 d 5	Direct velocity	F. Kirchner	Ann. d. Physik <b>8</b> , 975 (1931); <b>12</b> , 503 (1932)	"	
	1.7582	5 d 6	Crossed fields	A. E. Shaw	Phys. Rev. <b>54</b> , 193 (1938)	"	
	1.7580	5 s 7	Spectroscopic H <sup>1</sup> H <sup>2</sup>	C. D. Shane and F. H. Spedding	Phys. Rev. <b>47</b> , 33 (1935)	"	
	1.7578	5 s 8	Spectroscopic H <sup>1</sup> H <sup>2</sup>	R. C. Williams	Phys. Rev. <b>54</b> , 568 (1938)	"	
	1.7570	5 s 9	Zeeman effect	L. E. Kinsler and W. V. Houston	Phys. Rev. <b>45</b> , 104; <b>46</b> , 533 (1934)	"	
	$e^2/(mh)$	$3.82155 \times 10^{34}$	6	Magnetic deflection of x-ray photoelectrons	H. R. Robinson	Phil. Mag. <b>22</b> , 1129 (1936)	Robinson
3.8194		6	G. G. Kretschmar		Phys. Rev. <b>43</b> , 417 (1933)	Kretschmar	

scales of  $e$ ,  $m$  and  $h$  with a dot and dash line as in Fig. 2 to avoid confusion. For any desired point in the diagram about which two or more traces are consistent one may quickly read off the values of  $e_0$ ,  $m_0$  and  $h_0$  by scaling with dividers the distance from the point in question to each of the three dot-and-dash origin traces. The distance so scaled is then transferred with the dividers to its appropriate scale and read off immediately.

The *relationships* between different types of determination can be seen at a glance. For example note that the directions of the scales of  $e$ ,  $m$  and  $h$  do not differ greatly on the chart, and that the class of determination that comes nearest to this same general direction (other than the direct determination of  $e$  itself) is the class  $h/e$ . Next to  $h/e$  the class  $h/(em)^{\frac{1}{2}}$  (so far studied only by von Friesen) comes nearest to having this general direction, while  $e/m$  possesses this property perhaps least of all. This means that if we accept the Bohr-Rydberg relationship and the numerical value of the Rydberg as part of our data to be used simultaneously along with other experiments then the best or most crucial type to choose for determining  $e$ ,  $h$  and  $m$  is one which measures  $h/e$ . Next to this comes  $h/(em)^{\frac{1}{2}}$  while  $e/m$  need be known with very little precision if it is to be used for this purpose in conjunction with either of the two previous experiments.

The above statement is only a rough way of perceiving these relationships of course. In any precise consideration of the degree of dependence of  $e$ ,  $m$  and  $h$  on the various types of determination the size of the scale units (relative variation) for each function naturally plays a role as well as the slopes of the lines.

An advantage of the isometric chart here described is the relatively good independence of the different traces from each other and the resulting facility with which one can see the effect of a change in any single measurement or assumption including the value of  $R_{\infty}$ . The choice of the projection is such that even if the functional form of the Bohr-Rydberg formula were modified, only one really significant set of traces (Bäcklin, Bearden and Söderman) would have to be reorientated (for at the present the experi-

mental values of  $\alpha$  and  $\sigma$  cannot be regarded as having much meaning).<sup>9</sup>

The values themselves depicted in Fig. 2 have been modified and extended since the charts published in I NC as follows: The values of  $e/m$  from the different sources have been taken from a letter dated August, 1939, privately circulated by R. T. Birge who recomputed these values with the latest auxiliary constants.<sup>10</sup> The general aspect of the  $e/m$  band remains, however, about as before. The x-ray values of  $e$  (Bäcklin, Bearden and Söderman) are also modified very slightly from Birge's recomputation with the new auxiliary constants. No value of  $\sigma$  has been plotted since it would fall in a region very far off the chart.<sup>11</sup> The  $h/e$  values have been recom-

<sup>9</sup> The author is indebted to Professor Birge for pointing out to him a misleading statement on page 155 of I NC. It is stated that "the well-known Birge-Bond diagram has two disadvantages" . . . "(1) The data are treated in an arbitrary asymmetrical way (certain of the determinations are mixed with Eq. (7) while others are not) so that it becomes difficult to foresee (without replotting) the result of certain changes either from theory or experiment; (2) Relative variations of the same magnitude appear to very different scales on different ordinates." In an effort at brevity two ideas were rather carelessly confused in one sentence here. The arbitrary asymmetry referred to in the B-B diagram is really that one singles out one of the three variables to plot as ordinate (e.g.,  $e$ ) while another one (e.g.,  $h$ ) appears as the slope of a line on the graph and the third variable (e.g.,  $m$ ) does not appear at all because in all the determinations involving that variable the Bohr-Rydberg formula has been used to eliminate it. The present isometric chart lays no especial emphasis on any one of the three variables  $e$ ,  $m$  or  $h$  and they can all be made to appear explicitly on scales in a precisely similar way. So much for the "arbitrary asymmetry." The fact that certain of the determinations are mixed with the Bohr-Rydberg equation while others are not is indeed strictly true on both types of chart with the practical difference, however, that many more points on the B-B chart (in its present familiar form) than lines on the isometric chart are so mixed in the present state of what constitutes the interesting determinations. The quoted sentence from I NC implies that the mixture of certain determinations with Eq. (7) is a consequence of the arbitrary asymmetrical treatment when in fact it is a consequence of the effort to represent three variables in two dimensions. The author regrets and wishes to retract this incorrect implication.

<sup>10</sup> The principal change is in the value of  $q$ , the ratio of the size of international and absolute units of current as explained by Birge in his August, 1939, letter. This has been changed from  $q=0.99993$  to  $q=0.99986$  (J. Research Nat. Bur. Stand. 22, 485 (1939)). This affects the value of the faraday, the value of  $pq$  (factor to change from international to absolute volts) and, of course, consequently many other constants. The new value of  $q$  ends a discrepancy of long standing with the Nat. Phys. Lab. (England) and is very satisfactory, Birge reports.

<sup>11</sup> For a critical review of determinations of  $\sigma$  see F. G. Dunnington's excellent article, Rev. Mod. Phys. 11, 72 (1939). That author obtains an average value  $5.775 \times 10^{-5}$  from six sources, a value which, as can easily be seen from the scale of our Fig. 2, falls far off the diagram.



puted by the author to take account of these same slight changes and to correct a slight error on the previous chart all of which, however, makes no essential difference in the general aspect of the  $h/e$  band. To this band has also been added information from H. T. Wensel of the National Bureau of Standards who has kindly supplied the author in a private letter with a most interesting computation of  $h/e$  based on measurements of the constant  $c_2$  by optical pyrometric methods.<sup>12</sup> Professor F. Kirchner of Cologne, who has adopted the isometric chart to depict the consistency situation in his recent survey of the atomic constants,<sup>13</sup> has been so kind as to point out to the author the necessity for two modifications, one in each of the  $h/m$  determinations. The value of  $h/(em)^{\frac{1}{2}}$  recomputed by the author from von Friesen's data given in his dissertation remains practically as in INC save for slight modifications occasioned by the changed auxiliary constants. The same is true of Robinson's results on  $e^2/(mh)$ . To this function has also been added the results of Kretschmar who has reexamined his plates and recomputed his results which he kindly supplied in a recent letter to the author. It is interesting to note the good agreement between these two workers on this last mentioned precision experiment. The much less accurate work on  $h/e$  from the optical photoelectric effect<sup>14</sup> and from ionization potentials<sup>15</sup>

is merely added to the continuous x-ray limit work to show how it supports the general trend of the  $h/e$  results to be lower than one expects for consistency with the remainder of the diagram. Wensel's computed result which should have very considerable reliability and which is obtained by a method quite radically different from the short wave-length limit of the continuous x-ray spectrum also supports the latter work in giving  $h/e$  too low. The discrepancy thus remains as baffling as ever. The conclusions in INC remain unchanged.

#### PRACTICAL METHODS OF CONSTRUCTION

The actual construction of the isometric chart is very simple.<sup>16</sup> From the symmetry of the space diagram (Fig. 1, INC) the scales of percent variation of  $e/m$ ,  $h/e$  and  $h/m$  forming the sides of the hexagon are evidently of identical size. The range of  $\pm 0.5$  percent for each side of the hexagon seems to work out well in the present state of precision. For the mere mechanics of drafting alone it is, from this point on, unnecessary to think of the three-dimensional origin. The remaining two cozonal scales are laid out as follows. We may choose for example  $e/m$  and  $h/e$  (or more conveniently the relative deviations of these variables) as two independent variables whose specification fixes the position of any point on the chart. Now since  $h/(em)^{\frac{1}{2}} = (h/e)(e/m)^{\frac{1}{2}}$  it is evident that an *increase* of 0.5 percent in  $h/e$  and a *decrease* of 1.0 percent in  $e/m$  leaves  $h/(em)^{\frac{1}{2}}$  unchanged and such a variation therefore defines the direction of the trace  $h/(em)^{\frac{1}{2}} = h_0/(e_0m_0)^{\frac{1}{2}}$  which passes through the zeros of the percent scales for this function. But starting from the origin in the center of the chart an *increase* of 0.5 percent in  $h/e$  and a *decrease* of

<sup>12</sup> Wensel's computations are essentially those described in his paper "International temperature scale and some related physical constants," (H. T. Wensel, J. Research Nat. Bur. Stand. 22, 386-387 (1939)) save that a knowledge of  $c_2$  (see his Table 4) is used to compute  $h/e$  by his Eq. (14). In his communication to the author Wensel has computed a weighted mean  $c_2$  with the same numerical result as the unweighted mean of his Table 4. The procedure here of plotting an average value is admittedly inconsistent with the author's policy of showing independent determinations. It is necessitated in this case by the already large number of lines in the  $h/e$  band.

<sup>13</sup> F. Kirchner, *Die Atomaren Konstanten, Ergebnisse der Exakten Naturwissenschaften* (Julius Springer, 1939), Vol. 18.

<sup>14</sup> R. A. Millikan, *Electrons (+ and -), Protons, Photons, Neutrons and Cosmic Rays* (University of Chicago Press, 1935), p. 242, also Phys. Rev. 7, 362 (1916); P. Lukirsky and S. Prilezaev, *Zeits. f. Physik* 49, 248 (1928); A. R. Olpin, Phys. Rev. 36, 284 (1930); From Fig. 34 it is certain that Millikan used the conversion factor 300 instead of 299.776 to obtain the voltage in e.s.u. and it is highly likely that the same was true of the other two authors, hence I have taken the liberty of correcting all three of the above results for this. Each of these authors gives a value of  $h$  rather than  $h/e$  and from the dates of each work I have therefore, in recomputing back to find  $h/e$ , used, respectively,  $e=4.774$ ,  $4.774$  and  $4.770$ .

<sup>15</sup> E. O. Lawrence, Phys. Rev. 28, 947 (1926). L. C.

van Atta, Phys. Rev. 38, 876 (1931); 39, 1012 (1932). R. Whiddington and E. G. Woodroffe, Phil. Mag. 20, 1109 (1935). Here I have adopted Dunnington's recomputed values Rev. Mod. Phys. 11, 72 (1939).

<sup>16</sup> Since the appearance of the work of Beth and of DuMond, R. T. Birge has developed, very elaborately, tables giving analytic expressions for the relative sizes of scale units and angles, etc., etc., which amount, as he points out, to precise directions for constructing a variety of charts both of the type here described and of the Birge-Bond type. These analytic expressions, while interesting, give the impression that such charts are rather tedious and difficult to construct and that extensive computations may be involved. In practice, however, the construction of a chart can be done very simply and accurately by graphical means as here explained.

1.0 percent in  $e/m$  corresponds to a displacement to the lower right-hand corner of the hexagon. Thus the zero axis or trace for the percent scale of  $h/(em)^{\frac{1}{2}}$  must pass through the upper left and lower right corners of the hexagon and the scale of  $h/(em)^{\frac{1}{2}}$  is most conveniently laid out normal to this direction. Suppose we wish to have this scale cover a range of  $\pm 0.5$  percent. Evidently a displacement of the percent deviation of  $h/e$  from zero to  $+0.5$  percent, with  $e/m$  maintained at its origin value, will increase  $h/(em)^{\frac{1}{2}}$  just  $+0.5$  percent. On the chart the point where the percent variations of  $e/m$  and  $h/e$  have the respective values 0 and 0.5 percent fixes the distance of the  $+0.5$  percent trace for  $h/(em)^{\frac{1}{2}}$  from the zero percent trace for that function. It is elementary drafting procedure to construct the point in question and project it on the scales of  $h/(em)^{\frac{1}{2}}$  which can then be divided and subdivided into the appropriate number of parts. The procedure for  $e^2/mh$  follows exactly the same outline.

Now, however, for the noncozonal scales the procedure differs only very slightly from the preceding as was very briefly indicated in a footnote in INC (page 158). Each noncozonal function  $F$  can always be made to satisfy an identity of the form

$$(h/e)^i (e/m)^j \equiv (c/2\pi^2) R_{\infty} F^k.$$

Upon substituting the Bohr expression for  $R_{\infty}$  into this identity it is possible to solve for  $i$ ,  $j$  and  $k$ . An example is  $F=h$

$$(h/e)^{-5} (e/m)^{-1} = (c/2\pi^2) R_{\infty} h^{-2}.$$

This calls for a double scale on which variations of  $R_{\infty}$  with  $h$  constant and of  $h$  with  $R_{\infty}$  constant are to appear. Evidently the zero axis for percent variations of  $R_{\infty} h^{-2}$  corresponds to percent variations of  $h/e$  one-fifth as great and of opposite sign as the variations in  $e/m$ . Thus the zero axis

can be graphically constructed just as explained before and the axis of the  $R_{\infty} h^{-2}$  scale is laid out normal to this direction. Here, evidently, we see from the exponents in the above equation that holding the percent value of  $e/m$  at zero a decrease of 0.8 percent in  $h/e$  will produce an increase of 4.0 percent in  $R_{\infty}$  ( $h$  constant) or a decrease of 2.0 percent in  $h$  ( $R_{\infty}$  constant). Thus the displacement and sense for the ranges  $R_{\infty} = \pm 4.0$  percent,  $h = \pm 2.0$  percent on this scale are graphically constructed and the scale is divided up accordingly. These procedures suffice to construct scales for any type of function of  $e$ ,  $m$  and  $h$  desired.

The origin values should of course be computed for all the functions with considerably greater accuracy than any of the data of experiment. These on the present chart differ slightly from those in INC. They have been computed to be consistent with  $R_{\infty} = 109,737 \text{ cm}^{-1}$ . Once the origin value is known for any function it is a simple matter to construct a direct-reading scale for that function from the existing scale of relative deviation. A slide rule is amply accurate for computing the percent deviations corresponding to the decimal figures of the direct scale. The easiest procedure is to pick out two decimal figures each occurring near one of the ends of the direct-reading scale to be plotted, compute their corresponding percent deviations and plot them. Then by ordinary drafting technique carefully divide up the intermediate interval into the appropriate number of equal parts.<sup>17</sup>

<sup>17</sup> The author has prepared a master blank chart, to large scale, with considerable care, on tracing paper. This carries all the scales shown in Fig. 2 of this article but has no experimental results traced upon it. At a small charge (50¢ each) for the cost of black line contact printing and postage this chart will be supplied to anyone desiring it. The dimensions are approximately 30×35 inches. The contact printing and developing process fortunately introduces quite negligible distortion. All the prints are carefully checked as regards this point.